INL/JOU-15-37508
Accepted Manuscript

Using the Sound of Nuclear Energy

Steven Garrett, James Smith, Robert Smith, Brenden Heidrich, Michael Heibel

November 2016

The INL is a
U.S. Department of Energy
National Laboratory
operated by
Battelle Energy Alliance

Prepared for the U.S. Department of Energy
Office of Nuclear Energy
Under DOE Idaho Operations Office
Contract DE-AC07-05ID14517

RADIATION MEASUREMENT AND GENERAL INSTRUMENTATION

Using the Sound of Nuclear Energy

STEVEN GARRETT,[a] JAMES SMITH,[b] ROBERT SMITH,[c] BRENDEN HEIDRICH,[d] and MICHAEL HEIBEL[e]

KEYWORDS: Thermoacoustics, In-core sensing, wireless telemetry.

ABSTRACT

The generation of sound by heat has been documented as an "acoustical curiosity" since a Buddhist monk reported the loud tone generated by a ceremonial rice-cooker in his diary, in 1568. Over the last four decades, significant progress has been made in understanding "thermoacoustic processes," enabling the design of thermoacoustic engines and refrigerators. Motivated by the Fukushima nuclear reactor disaster, we have developed and tested a thermoacoustic engine that exploits the energy-rich conditions in the core of a nuclear reactor to provide core condition information to the operators without a need for external electrical power. The heat engine is self-powered and can wirelessly transmit the temperature and reactor power level by generation of a pure tone which can be detected outside the reactor. We report here the first use of a fission-powered thermoacoustic engine capable of serving as a performance and safety sensor in the core of a research reactor and present data from the hydrophones in the coolant (far from the core) and an accelerometer attached to a structure outside the reactor. These measurements confirmed that the frequency of the sound produced indicates the reactor's coolant temperature and that the amplitude (above an onset threshold) is related to the reactor's operating power level. These signals can be detected even in the presence of substantial background noise generated by the reactor's fluid pumps.

[a] Graduate Program in Acoustics, Penn State University, University Park, PA 16802; sxg185@psu.edu.
[b] Fundamental Fuel Properties, Idaho National Laboratory, Idaho Falls, ID 83415.
[c] Applied Research Laboratory, Penn State University, State College, PA 16804.
[d] Nuclear Science User Facilities, Idaho National Laboratory, Idaho Falls, ID 83415.
[e] Nuclear Measurement Methods and Applications, Westinghouse Electric Company, Pittsburgh, PA 15235.

I. MOTIVATION

Amazing progress has been made in the worldwide acceptance of solar and wind power, but those environmentally benign "clean" electrical power sources are intrinsically intermittent. New energy storage technologies and improved and geographically dispersed power grids must be developed to provide "load leveling."[1] Both of those approaches are at least a decade away from widespread commercialization.

Other than hydroelectric generation, nuclear power is the only existing technology that is both carbon-free and continuously available. Nuclear power is not limited by topographical constraints, unlike hydroelectric generation. As the Fukushima disaster demonstrated, it is also a technology that does not mix well with water. All six of the reactors at the Fukushima Daiichi facility survived the largest recorded earthquake in Japanese history. The situation was under control until the tsunami arrived, about 45 minutes later, with a maximum wave height of approximately 15m (three times taller than the sea wall). The influx of sea water submerged the emergency generators, the electrical switchgear, and DC back-up batteries, resulting in the total loss of power to five of the six reactors.[2] This in turn resulted in the complete loss of instrumentation that could have otherwise been used for monitoring and control during that emergency. Similar circumstances could result in the flooding of reactors on the California coast or at the surprisingly large number of nuclear reactors in the U.S. that are down-stream from hydroelectric dams.[3] Thermoacoustic sensors of the type we tested could continue to supply temperature and power information in such an emergency.

Under normal reactor conditions, multiple thermoacoustic sensors operating at different acoustic resonance frequencies, placed at several locations within the reactor's core, could also be utilized to provide information to reactor operators to optimize the production of electrical power. The recent irradiation test at the Breazeale Nuclear Reactor at The Pennsylvania State University utilized two UO_2 pellets as the heat source for the thermoacoustic engine. In most circumstances, it would be preferable to provide the engine's heating by gamma-ray absorption, rather than the fission of ^{235}U nuclei, since strong gamma absorbers, like tungsten and stainless steel, do not require special handling and material inventory controls, and can be transported by common carriers. Additionally, gamma absorbers do not become depleted. Unfortunately gamma heating was not practical at the Breazeale Nuclear Reactor because the gamma fluxes were too weak in a 1MW university TRIGA research reactor. In a commercial power reactor, the heating available in the reactor core from gamma absorption is on the order of 5 W/gm or more for gamma-absorbing materials.

II. THERMOACOUSTIC SOUND PRODUCTION

The generation of sound by heat has been documented as an "acoustical curiosity" since a Buddhist monk reported the loud tone generated by a ceremonial rice-cooker in his diary, in 1568.[4] The Sondhauss tube[5] is the earliest thermoacoustic engine that is a direct antecedent of the self-powered sensor that we developed and tested. In 1850, Karl Friedrich Julius Sondhauss documented and investigated an observation made by glassblowers who noticed that when a hot glass bulb was attached to a cool glass tubular stem, the stem tip sometimes emitted sound.[6]

The first qualitative explanation of the Sondhauss effect was provided by Lord Rayleigh: "If heat be given to the air at the moment of greatest condensation or be taken from it at the moment of greatest rarefaction, the vibration is encouraged."[7] As proven by our experiment, the new thermoacoustic sensor automatically does both. The standing sound wave transfers heat from the solid substrate to the gas (in our case a mixture of helium and argon rather than air) at the phase of the acoustic cycle during which the condensation (*i.e.*, density and pressure) is maximum and removes heat from the gas and deposits it on a solid substrate (at a different location) at the phase of the cycle when the condensation is a minimum.

In this process, illustrated schematically in Fig. 1, the sinusoidal variation in the gas's pressure and density at any location is replaced, to simplify the description, by a four-step articulated cycle analogous to a four-cycle automotive engine. Adjacent layers of the solid substrate are separated by several thermal penetration depths,[8] δ_κ, which is approximately the length scale over which heat can diffuse during one-half of an acoustic period, $T/2 = (2f)^{-1}$.

$$\delta_\kappa = \sqrt{\frac{\kappa}{\pi \rho_m c_P f}} \tag{1}$$

The gas's thermal conductivity, mean mass density, and specific heat at constant pressure are κ, ρ_m, and c_P. For our experiment, the gas is a mixture of 25% argon and 75% helium at a mean pressure, p_m = 2.0 MPa, and $f \cong$ 1,350 Hz, making $\delta_\kappa \cong$ 50 microns.

During the first quarter-cycle, a macroscopic parcel of gas that is in thermal equilibrium with the substrate at temperature, T_o, moves toward the closest rigid end of the resonator and is compressed. That compression is approximately adiabatic (since the gas does not have time to come to equilibrium with the substrate); hence, the increase in the parcel's temperature, δT, is related to the increase in pressure, δp. The mean gas temperature is T_m and the mean gas pressure is p_m.

$$\delta T = \left(\frac{\gamma - 1}{\gamma} \right) \frac{\delta p}{p_m} T_m \tag{2}$$

The ratio of the gas's specific heat at constant pressure to its specific heat at constant volume is $\gamma = c_P/c_V$. For an inert gas or inert gas mixture, γ = 5/3; for diatomic gases, γ = 7/5. Conceptually, in the notation that follows, an increase in the number of '+' subscripts to the temperature, T, represents higher temperature, in arbitrary units, and the addition, or subtraction of a '++' represents the temperature increase or decrease associated with an adiabatic pressure change. Thus, in Fig. 1, that adiabatic temperature increase, δT, is represented by the change in the parcel's temperature from T_o to T_{++}, as it moves through the first step of the articulated cycle.

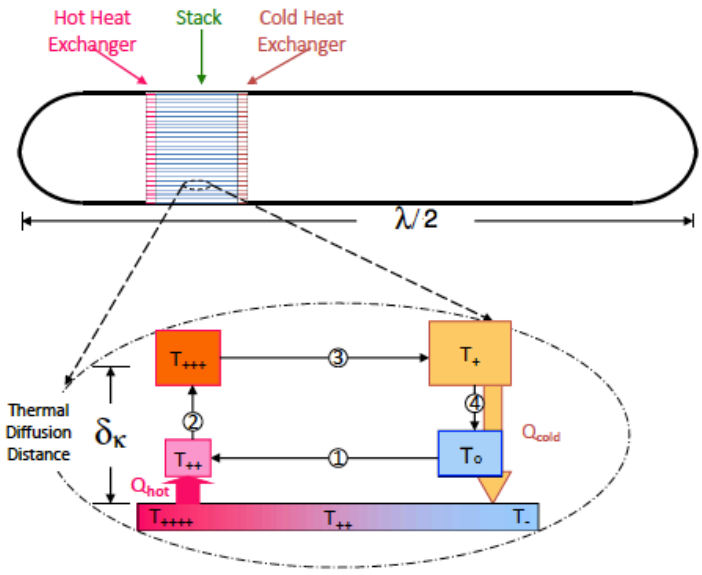

Fig. 1. Simplified Lagrangian representation of the thermoacoustic process that converts a temperature gradient imposed on a solid substrate (stack) to the maintenance of an acoustic standing wave in the gas contained within a sealed resonator. The "stack" can be represented by a stack of parallel plates that have a heat capacity that is much greater than the gas and are separated by a distance, $2y_o$, which is several times the thermal penetration depth, $\delta_\kappa \ll y_o$.

During the second quarter-cycle, the gas parcel is temporarily at rest and in good thermal contact with the substrate, which is hotter than the gas. The substrate's temperature at that location is indicated as T_{++++}. Since the parcel is cooler than the substrate, an amount of heat, Q_{hot}, flows from the substrate to the gas parcel, raising its temperature to T_{+++}, thus fulfilling the first part of Lord Rayleigh's criterion for the maintenance of the acoustic oscillation (*i.e.*, the conversion of a temperature gradient to mechanical work in the form of the standing sound wave) by adding heat "at the time of greatest condensation."

During the third quarter-cycle the gas moves away from the closest rigid end, its pressure decreased by δp, and it is cooled adiabatically, according to Eq. (2), so its temperature is decreased from T_{+++} to T_+. During the fourth quarter-cycle, the gas parcel is again temporarily at rest and finds itself over a portion of the substrate that is cooler, so an amount of heat, Q_{cold}, is transferred from the gas parcel at T_+ to the substrate at T_o, thus completing the

cycle and fulfilling the second part of Lord Rayleigh's criterion by removing heat "at the time of greatest rarefaction."

Typically the stack is many acoustic displacements long, and the adiabatic temperature fluctuation for a parcel of gas, per Eq. (2), is a modest fraction of the mean (absolute) gas temperature, T_m. Using this Lagrangian perspective, the thermoacoustic process can be seen as a "bucket brigade" that is transferring heat from the hot end of the stack to the cooler end of the stack while doing useful work on the gas in the process. The hot heat exchanger replaces the heat on the hot end and the cold heat exchanger removes the exhaust heat (at a lower temperature) from the cold end.

It is worthwhile to point out that this is an extremely simple engine cycle when compared to an automobile engine that requires pistons, valves, cams, rocker-arms, a flywheel, etc. to have the compressions and expansions occur at the proper phases in the cycle. By contrast, this thermoacoustic process is phased by a natural process (thermal diffusion) and requires no moving parts other than the oscillatory motion of the gas. The irreversibility of the diffusion process reduces efficiency from that achievable using a traveling-wave thermoacoustic-Stirling cycle,[9] but in the energy-rich core of a nuclear reactor, efficiency is less important than simplicity.

In a gas-filled resonator of length, L, that is excited in its fundamental standing-wave mode, the boundary conditions at the ends, $x = 0$ and $x = L$, require that the longitudinal gas velocity, $v_1(x, t)$, vanish, since the gas cannot pass through those ends. The oscillatory pressure, $p_1(x, t)$, is related to that velocity by the linearized Euler equation: $\partial\vec{v} / \partial t = -\vec{\nabla}p / \rho$.[8]

$$v_1(x,t) = v_1 \sin\left(\frac{\pi x}{L}\right)\cos(\omega t) \quad \text{and} \quad p_1(x,t) = \rho_m c v_1 \cos\left(\frac{\pi x}{L}\right)\sin(\omega t) \tag{3}$$

The speed of sound in the gas is c and ρ_m is again the mean density of the gas. If the partial obstructions to the flow due to the stack and heat exchangers are ignored, the frequency of the first fundamental resonance, f, corresponds to one-half wavelength, $\lambda/2$, of the sound being equal to the length of the resonator: $f = \omega/2\pi = c/\lambda = c/2L$.

The displacement of a gas parcel is in time-quadrature with the gas velocity and its magnitude is given by $|x_1(x, t)| = |v_1(x, t)|/\omega$. Using the adiabatic temperature lapse of Eq. (2) and the expressions for the standing wave's oscillatory particle velocity and pressure in Eq. (3), a critical temperature gradient, $(\nabla T)_{crit}$, can be calculated as the ratio of the magnitude of the oscillating temperature, $|T_1(x, t)|$, to the magnitude of the oscillatory gas parcel displacement, $|x_1(x, t)|$.

$$(\nabla T)_{crit} \equiv \frac{|T_1(x,t)|}{|x_1(x,t)|} = 2\pi\frac{(\gamma-1)}{\gamma}\frac{T_m}{\lambda}\cot\left(\frac{\pi x}{L}\right) \tag{4}$$

When the temperature gradient along the stack, ∇T_m, exceeds the critical value, then the system becomes unstable and the resonant sound wave is amplified while additional heat is transported along the stack hydrodynamically by the sound wave. The amount by which ∇T_m must exceed $(\nabla T)_{crit}$ is determined by the need to overcome the ordinary thermoviscous dissipation within the resonator and the thermoacoustic components it contains (*i.e.*, stack and heat exchanger).

Although easy to explain, this simple Lagrangian model is not well suited to the calculation of heat transport and acoustical energy production in actual thermoacoustic engines. An Eulerian formalism was developed by Nikolas Rott and co-workers who published an incredible series of papers starting in 1969,[10] and introduced the term "thermoacoustics," claiming that it was self-explanatory. Rott's theoretical approach was developed further and applied to design and analysis of thermoacoustic engines and refrigerators by Swift and his co-workers at the Los Alamos National Laboratory.'[11]

III. IN-CORE "FUEL ROD" THERMOACOUSTIC SENSOR

The thermoacoustic sensor we describe, which converts the heat of ^{235}U fission to a standing sound wave, is fundamentally no more complicated that the simple schematic representation in Fig. 1. The entire sensor system was designed to have a size and shape that is identical to the TRIGA fuel rods in the Breazeale Nuclear Reactor shown in Fig. 2. Those fuel rods have a maximum external diameter of 3.7 cm and an overall length of 72 cm. Like the reactor's fuel rods, the sensor had a centering pin at the bottom for positive positioning in the bottom grid of the core (see Fig. 2, bottom, far right) and a "pull-pin" at the top, so it could be inserted and removed from the reactor's core using the same tool that is used for insertion and removal of the fuel rods.

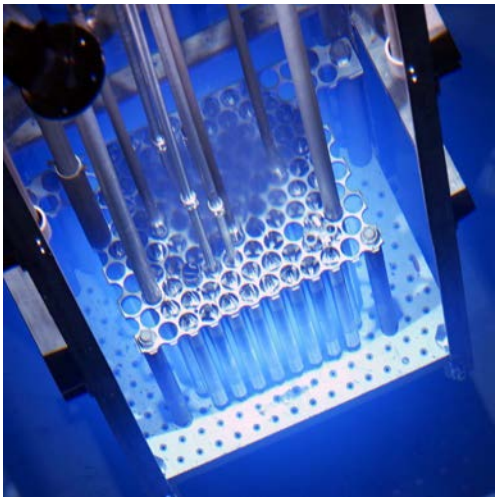

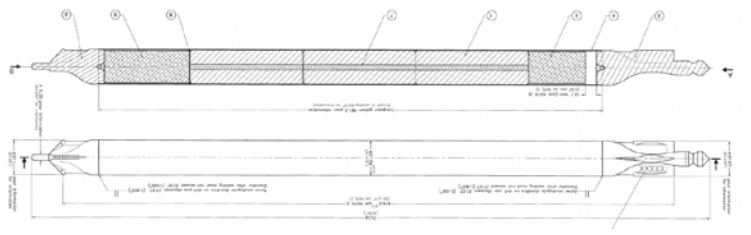

Fig. 2. Fuel rods used in the Breazeale Nuclear Reactor. (Left) Photograph of the reactor's core. (Upper right) Several fuel rods. (Lower right) Cross-sectional drawings of fuel rods.

The high-amplitude acoustic standing wave that is generated thermoacoustically causes the gas in the "empty" section of the resonator to be pumped by nonlinear acoustic forces that create streaming cells.[12] This acoustically-induced flow forcibly convects heat from the ambient-temperature of the end of the stack to the walls of the resonator that are bathed in the reactor's cooling water. Measurements have shown that this streaming flow increases the thermal contact between the ambient-temperature end of the stack and the coolant by a factor-of-three in a similar "fuel rod" resonator.[13] This makes our thermoacoustic sensor, shown in Fig. 3, even simpler than the version shown in Fig. 1 because no physical "cold heat exchanger" is required.

When an acoustic standing wave is excited in the resonator, the gas "sloshes" back and forth along the axis of the resonator and the momentum of that oscillatory gas motion causes the resonator's body to vibrate in reaction, also along the axis of the slotted tube. The oscillatory motion of the resonator radiates a dipolar sound field into the surrounding coolant fluid. In a free-field environment, the total radiated acoustic power, Π, depends upon the force, F_1, which the oscillating gas exerts on the resonator of volume, V_{res}, on the moving mass of the resonator and the entrained mass of the surrounding fluid,[14] m_{res}, and on the mass density and speed of sound in the water surrounding the resonator, ρ_{H_2O} and c_{H_2O} .[15]

$$\Pi = \frac{\rho_{H_2O}\omega^2 V_{res}^2}{12\pi c_{H_2O}^3}\left(\frac{F_1}{m_{res}}\right)^2 \tag{5}$$

Of course, an oscillating dipole in a "slotted tube" placed in a 70,000 gallon pool of water with half-meter thick concrete walls does not exactly duplicate "free-field" acoustic radiation conditions.

Fig. 3. "Fuel rod" thermoacoustic sensor. (Above) The thermoacoustic resonator is shown at the center of the photograph. The resonator tube has an inside diameter of 2.2 cm and is 22 cm long. The hot section of the resonator holds the hot heat exchanger that contains two enriched ^{235}U fuel pellets that are each approximately 5 mm in diameter and 10 mm long, as well as the extruded ceramic "stack." The hot section is surrounded by an insulation tube with an outside diameter of 3.0 cm, which is about 7.5 cm long, containing a SiO_2 floss. That insulation space is filled with air at atmospheric pressure. The remainder of the resonator tube is empty other than containing the 2.0 MPa mixture of 75% He and 25% Ar that fills the entire resonator. The empty portion of the resonator has a 0.51 mm wall thickness and is in good thermal contact with the reactor's coolant water. The two 4-40 threaded rods that extend from either end of the resonator are attached to two circular stainless steel (SS) disks that are 200 microns thick and have six spokes that act as cantilever springs to allow the resonator to vibrate axially but constrain the resonator to remain coaxial within the surrounding "slotted tube." The rings that clamp the periphery of the springs are each welded to three SS rods to facilitate insertion into the slotted tube after assembly. Exiting the insulation tube at the left are two Type-K thermocouple (T/C) leads. One of the thermocouples is silver-soldered (brazed) to the thin-walled section of the resonator next to the heat exchanger and the other is silver-soldered to the hot end of the resonator. Both T/Cs are located within the insulation space. A rhodium neutron flux sensor, with a sensing length of 9.8 cm, is coiled in the space between the end of the insulation tube and the adjacent spring. (Below) The resonator and springs are contained within a "slotted tube" that has the same outer diameter as the fuel rods. The slots allow the reactor's coolant water to remove the heat of fission from the thermoacoustic sensor and facilitated testing of the resonator's axial mobility before insertion in the reactor's core.

IV. THE REACTOR'S VIBROACOUSTIC ENVIRONMENT

The detectability of the sound radiated by the thermoacoustic sensor depends upon the acoustics of the coolant pool and the vibroacoustic background noise level that is typically dominated by pumps used by the reactor to circulate coolant. In the Breazeale Nuclear Reactor, the dominant noise was created by a diffusor pump that is used to circulate coolant (light water) over the reactor to reduce the radiation level in the reactor bay from ^{16}N. Its primary function is to recirculate water above the core containing radioactive ^{16}N (which decays to ^{16}O with a 7.13 second half-life) and keep it well below the surface of the pool while it decays. That ^{16}N pump is automatically activated when the reactor power exceeds 180 kW (18% of full power).

Since the reactor pool, shown in Fig. 4, is a reverberant acoustical environment, we measured the standing-wave modal structure of the pool and the acoustic reverberation time.[16] Based on the equivalent rectangular dimensions of the reactor coolant pool (8.65 m long, 4.27 m wide, and 7.32 m deep), the lowest frequency standing-wave modal frequency is about 51 Hz. In a 3-dimensional enclosure, the number of modes below a given frequency increases with the cube of that frequency.15 At some frequency, there will be three modes with resonance frequencies overlapping within the half-power bandwidth of a single mode. That "overlap" frequency is known within the architectural acoustics community as the Schroeder frequency, f_S.[17] Above f_S, the sound field can be treated as being diffuse (*i.e.*, uniform energy density independent of the location of the source and the sensors) so the sound field can be approximated as a "phonon gas" and the sound pressure can be estimated using statistical energy analysis.

Based on our measurements of the reverberation time (T_{60} = 120 ± 20 ms → $\tau_E = T_{60}/\mathrm{Ln}[10^6] \cong 8$ ms), at the frequencies near the sensor's resonance frequency, f, we found $f_S \cong$ 230 Hz << $f \cong$ 1,350 Hz.[18] The sound field will then be uniform at measurement distances from the source greater than the critical radius, $r_d = c_{H_2O}/5f_S \cong 1.3\ \mathrm{m}$.[19] Under those acoustic conditions, the diffuse, time-averaged, steady-state, root-mean-squared acoustic pressure, p_r ($t = \infty$), produced by a dipole radiator (under free-field conditions), is related to the exponential relaxation time, τ_E, and the volume of the pool, V.

$$p_r\left(t=\infty\right) = c_{H_2O}\sqrt{\frac{\rho_{H_2O}\tau_E}{V}\Pi} \tag{6}$$

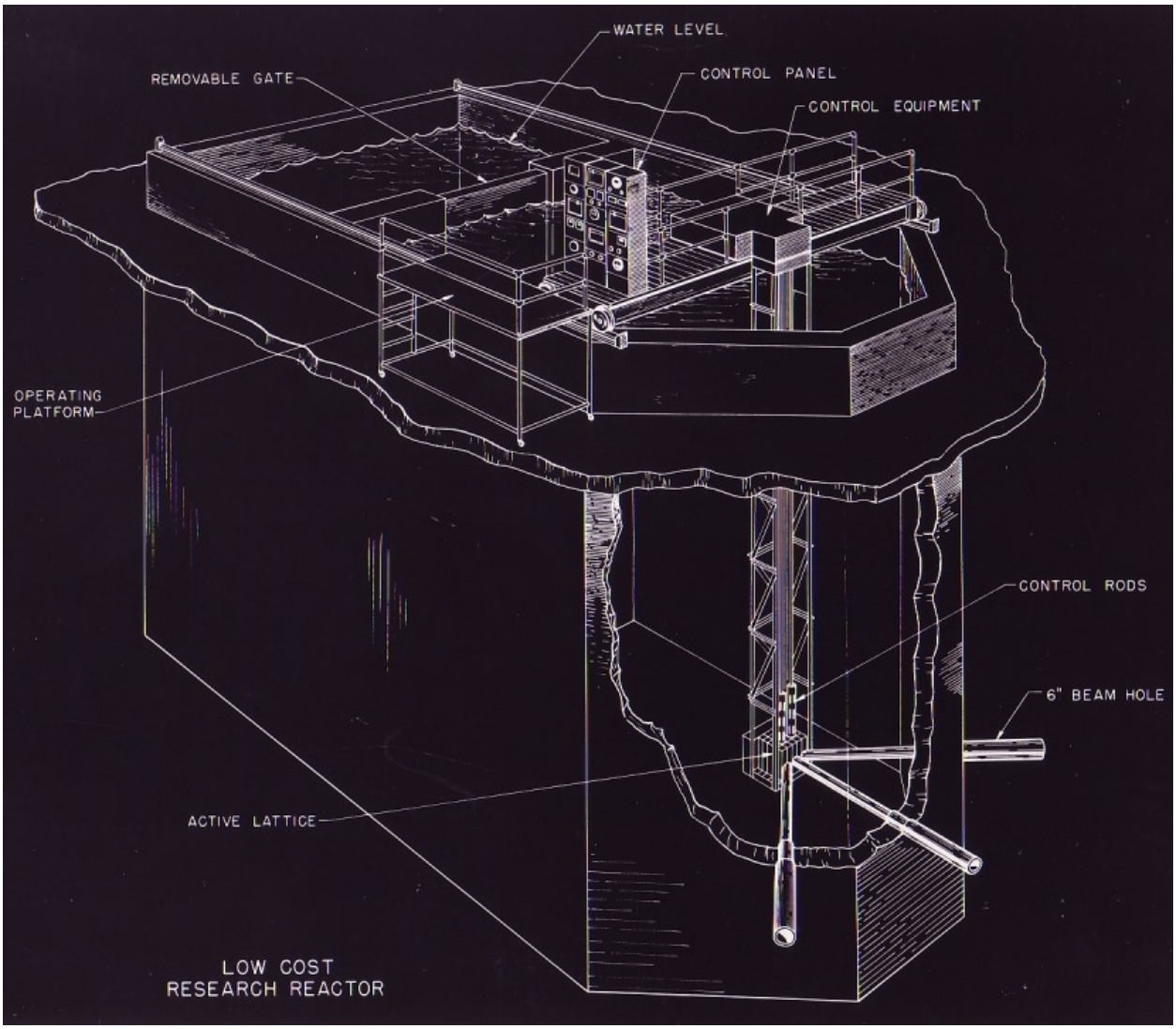

Fig. 4. Drawing of the Breazeale Nuclear Reactor's pool. This drawing was taken from the original 1953 proposal to build this research reactor on the campus of Penn State University.

V. REACTOR CORE *IN SITU* MEASUREMENTS

Our thermoacoustic sensor was tested during eight irradiation runs in the Breazeale Nuclear Reactor on Penn State's University Park campus. While the TRIGA reactor fuel is very robust and resistant to failure, experiments containing uranium and other nuclear fuel materials are limited by the safety basis. The sensor irradiations were restricted to an integrated power of approximately eight MW-minutes, due to the buildup of radioactive iodine in the fuel pellets that were used to heat the sensor. The enriched ^{235}U pellets that provided our fission heat source produces five major isotopes of radioactive iodine (^{131}I through ^{135}I) with half-lives ranging from 0.9 hours to 193 hours. The reactor was operated for each demonstration run while a separate computer calculated the radioiodine production in the fuel pellets in real time. Following each run, the experiment was idled while the iodine was allowed to decay. With the exception of the first and last day that our sensor was in the reactor's core, we irradiated for about six minutes in the morning and in late afternoon each day. Figure 5 shows the behavior of the radioiodine during a proposed testing schedule.

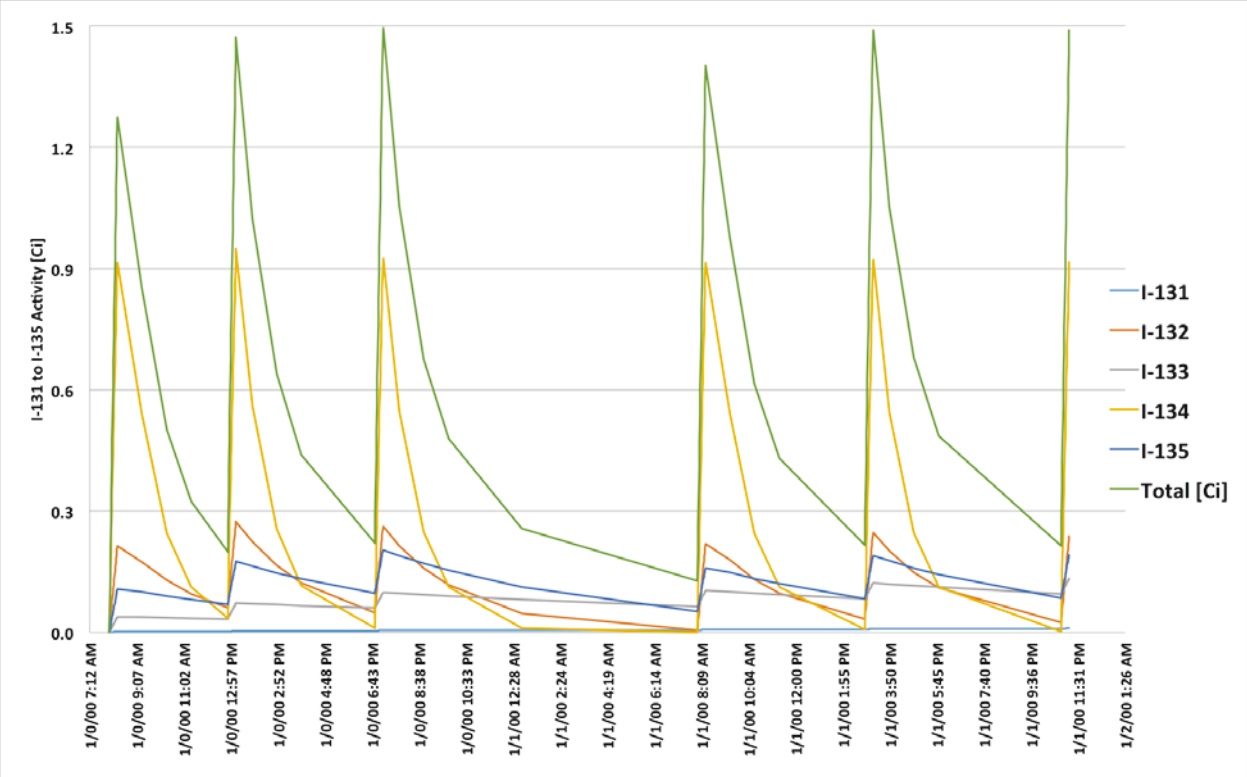

Fig. 5. Radioiodine production and decay during a proposed irradiation schedule. The graph shows three days of planned reactor operations.

Figure 6 is a time record made during the 5th irradiation. It shows the temperature of the thermocouple that was brazed to the rigid hot-end of the thermoacoustic resonator, contained in the insulation space, as well as the output of two hydrophones that were located in the reactor's pool. One hydrophone was placed above the reactor's core equidistant from the top of the core and the free-surface of the pool approximately 4 m from the core. The other hydrophone was placed as far from the core as possible, approximately 8 m from the core, close to the bottom of the pool. Due to the differences in their locations, they had different proximity to the sources of pump noise (*e.g.*, the over-core hydrophone was close to the outlet of the ^{16}N pump).

All hydrophone and accelerometer signals were digitized at 25,000 samples/second (16-bit) and recorded. Short Time Fast (essentially sliding-average) Fourier transforms with ten-second time records were produced every two seconds and the frequency of the largest-amplitude spectral component is plotted in Fig. 6 for both hydrophones. It is easy to see that the thermoacoustic sensor achieved onset at about t = 810 s, at which time the largest amplitude spectral components for both hydrophones coalesced. It is also possible to detect a subtle indication of the onset of thermoacoustic oscillations suggested by the slight increase of the slope of the thermocouple's temperature *vs*. time at that same instant. This indicated a hydrodynamically-enhanced increase in the uniformity of the distribution of the heat from the hot heat exchanger (which contains the two ^{235}U fuel pellets) to all other locations within the resonator.

Before onset of thermoacoustic oscillations (t < 810 s) and after their cessation (t > 1,100 s), the frequencies of the dominant spectral components from both hydrophones' signals are fairly random. This is as would be expected when only the pump noises were received within the displayed bandwidth, Δf = ±40 Hz.

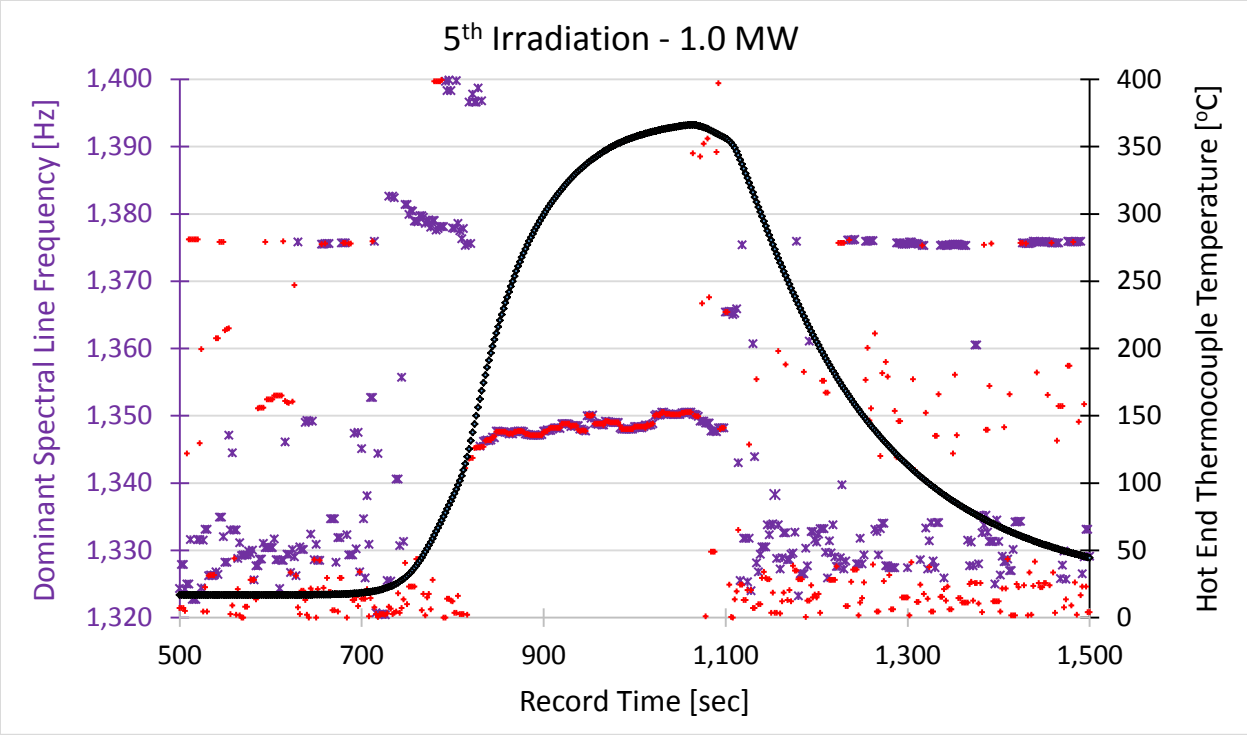

Fig. 6. **Time record of the temperature and the frequency of the largest spectral component received by two hydrophones at different locations.** The temperature of a Type-K thermocouple brazed to the hot-end of the thermoacoustic resonator is plotted as the black diamonds. Those temperatures should be read from the right-hand (black) axis. The blue "x" and red "*" symbols are the frequencies of the largest spectral component within the frequency range between 1,320 Hz $\leq f \leq$ 1,400 Hz. Those frequencies should be read from the left-hand (purple) axis. All data points are plotted every two seconds. The time axis is labeled from the start of the recording. The reactor reached full power (1.0 MW) at $t \cong$ 800 s. The reactor power was reduced to 800 kW at $t \cong$ 1,060 s, then the reactor was shut down at $t \cong$ 1,100 s, since fission had produced the maximum allowable amount of radioactive iodine.

Figure 7 shows one of several accelerometers that were attached to structures external to the reactor's coolant pool. The sonogram is taken from a 16-bit, 44.1 kilosamples/second digital audio recording and displays the frequency of the detected vibration as a function of time with the amplitude of the signal coded as color from blue to yellow. Because the characteristic impedance of the water is close to the impedance of the solid structures that penetrate the reactor pool, the sound produced by the sensor couples well to those structures. The ability for the thermoacoustically-generated sound to couple to reactor structures means that the sensor's signals do not have to be detected by hydrophones submerged directly in the reactor's coolant.

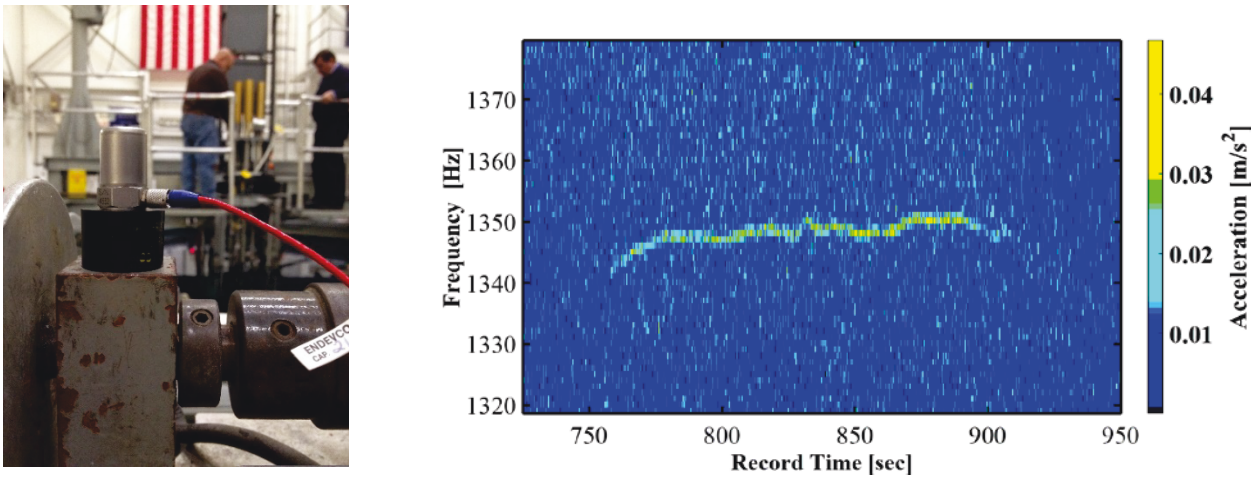

Fig. 7. Time record (spectrogram) of the vibration signal received by an accelerometer mounted on a structure outside the reactor pool. (Left) Accelerometer with a magnetic base (black) attached to the motor mount of an instrumentation tower that extends into the reactor pool. (Right) Spectrogram showing the accelerometer's output frequency on the vertical axis as a function of time represented by the horizontal axis. The amplitude of the accelerometer's output is encoded by color.

Due to the limitations imposed by the radioactive iodine regulatory restrictions, we were only able to demonstrate that the amplitude of the thermoacoustically produced sound which turned on and off for various reactor powers. Had the times of the irradiations been unrestricted, it would have been possible to allow the thermoacoustic resonator to reach its steady-state amplitudes at various reactor power settings. As demonstrated in Fig. 8, we were able to show that the frequency of the thermoacoustically-generated sound provides an accurate measurement of the reactor's coolant temperature.

The speed of sound, c, in an ideal gas or gas or ideal gas mixture is related to the acoustically-averaged absolute (Kelvin) temperature, T, the mean molecular mass of the gas, M, and the Universal Gas Constant, $\Re$ = (8.314472 ± 0.000015) J·mol^{-1}·K^{-1}.

$$c = \sqrt{\frac{\gamma \Re T}{M}} \tag{7}$$

The accepted value of $\Re$ was determined from a sound speed measurements in a spherical resonator[20] and the international definition of absolute temperature will also soon be based on sound speed measurements using acoustic resonators.[21]

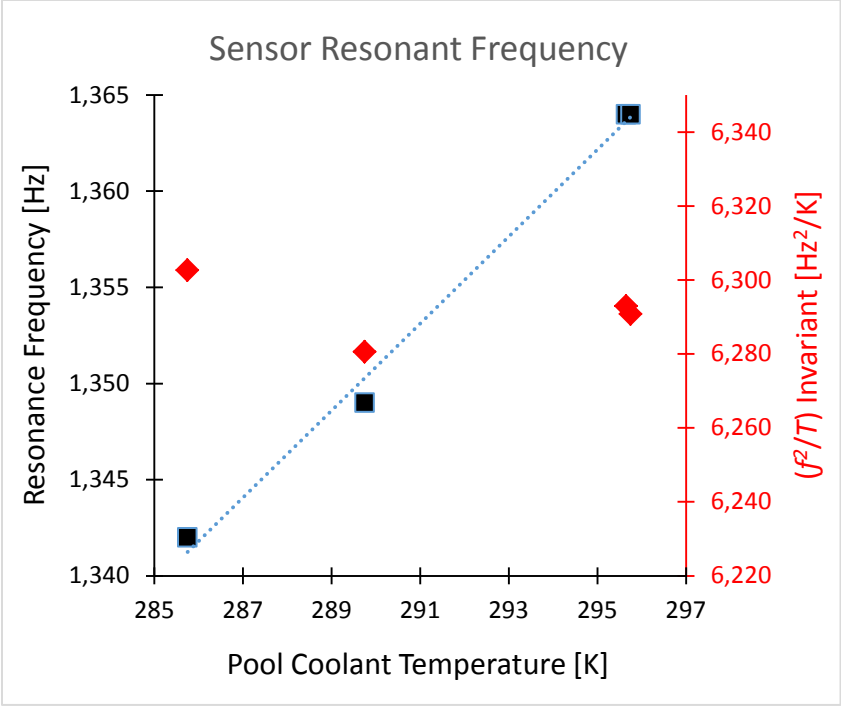

Fig. 8. Frequency of the thermoacoustic sensor's standing-wave. The sensor's resonance frequencies were measured at four different water temperatures between 12.6 °C and 22.6 °C in the reactor's 70,000 gallon (265 m^3) pool. The resonance frequencies corresponding to those temperatures are plotted as black squares and their values are given by the left-hand (black) axis that spans ±1.7%. The right-hand (red) axis has the same relative span, but the value of the f^2/T invariant, plotted as red diamonds, has a standard deviation of only ±0.12%.

Ignoring the small changes in the resonator's otherwise uniform cross-sectional area caused by the porous heat exchanger and stack, the fundamental resonance frequency of the thermoacoustic sensor occurs when the wavelength of the sound in the gas mixture, $\lambda = c/f$, is twice the length, L, of the resonator.

$$f^2 = \frac{c^2}{4L^2} = \frac{\gamma \Re T}{4ML^2} \propto T \tag{8}$$

The temperature of the gas mixture within the thermoacoustic resonator varies significantly from the high temperatures at the hot end (containing the heat exchanger) to about the temperature of the reactor coolant in the largest portion of the resonator between the ambient-temperature end of the stack and the ambient-temperature end of the resonator. A simple lumped-element model of the resonator as a "gas mass" at the center of the resonator surrounded by two "gas springs" suggests that the frequency is determined largely by the density of the lower temperature gas near the center of the resonator. The temperature of the central gas mass is controlled by the temperature of the reactor's coolant. A more detailed lumped-element model, treating the resonator as the concatenation of 31 lumped-elements, is able to provide a better estimate of the relationship between resonance frequency and coolant temperature.[22]

As is apparent from Fig. 8, just forming the ratio of the square of the measured resonance frequency, f^2, to the absolute (Kelvin) temperature, T, of the reactor's coolant, based

on Eq. (8), produces values of f^2/T that vary by only ±0.12%, while the temperature changes by 3.4%.

VII. CONCLUSION

A very simple heat engine has been described that was suitable for placement in the core of a nuclear reactor as a replacement for one of the reactor's fuel rods. The engine's heat source was two pellets containing low-enriched ^{235}U (7wt.%). Their heating produced thermoacoustic oscillations with an amplitude that was related to the reactor's operating power and a frequency that determined the temperature of the reactor's coolant. Those signals were detectable even in the presence of significant background noise. This acoustical information was wirelessly telemetered throughout the reactor and was detected on hydrophones in the coolant several meters from the reactor's core and on accelerometers attached to structures external to the reactor.

In a more powerful reactor, such as those used for commercial power plants, the heating could be provided by the absorption of gamma radiation rather than by neutron-induced fission. This would simplify production and handling of such thermoacoustic engines as self-powered, acoustically-telemetered, power and temperature sensors capable of operation in the cores of nuclear reactors. In the future, a reactor might contain several such sensors, each operating at a different frequency that would be determined by each resonator's length and/or gas mixture concentration, to produce a nuclear-powered "pipe organ" generating a chorus of sounds that could be used to optimize the reactor's operating point under normal conditions and provide potentially life-saving information about the reactor's operation under emergency conditions if electrical power became unavailable. This is not the obvious evolutionary path for a ceremonial rice cooker.

ACKNOWLEDGEMENTS

The design and optimization of this sensor relied on the Dynamic Environment for Low-Amplitude Thermoacoustic Energy Conversion (DELTAEC), a software package developed and supported over twenty-five years by G. W. Swift and W. W. Ward at the Los Alamos National Laboratory. The authors are grateful to the support of Larry Bodendorf, Iain Wilson, James Lynch, and Brandon Rieck of IST Mirion for fabrication of the resonator and for its fueling. We are also appreciative of the support provided by Penn State's Radiation Science & Engineering Center for ensuring that the experiment could be operated safely and in full compliance with all NRC regulatory limits. J. A. S. thanks James Lee and Keith Jewell for help with the assembly and testing of the data acquisition system and Vivek Agarwal for assistance with the data analysis. The participation of Randall Ali, Joshua Hrisko, and Andrew Bascom, three of S. L. G.'s former graduate students, who contributed to the success of these experiments, is also appreciated. This research was supported by the U.S. Department of Energy's Idaho National Laboratory and

by the Westinghouse Global Technology Development Department of the Westinghouse Electric Company.

REFERENCES

1. S. BACKHAUS and M. CHERTKOV, "Getting a grip on the electrical grid," *Phys. Today* **66**(5), 42-48 (2013).
2. D. KLEIN and M. CORRADINI, *Fukushima Daiichi: ANS Committee Report*. American Nuclear Society (Revised June 2012).
3. D. LOCHBAUM, E. LYMAN, and S. Q. STRANAHAN, *Fukushima: The Story of a Nuclear Disaster* (Union of Concerned Scientists, 2014); ISBN 978-1-59558-908-8.
4. D. NODA and Y. UEDA, "A thermoacoustic oscillator powered by vaporized water and ethanol," *Am J. Phys.* **81**(2), 124-126 (2013).
5. C. SONDHAUSS, "Über die Schallschwingungen der Luft in erhitzten Glasröhren und in geteckten Pfeifen von ungleicher Weite," *Ann. Phys. (Leipzig)* **79**, 1 (1850).
6. G. W. SWIFT, "Thermoacoustic engines," *J. Acoust. Soc. Am.* **84**(4), 1145-1180 (1988).
7. J. W. STRUTT (Lord Rayleigh), "The explanation of certain acoustical phenomena," *Nature* **18**, 319-321 (1878).
8. L. D. LANDAU and E. M. LIFSHITZ, *Fluid Mechanics*, 2nd ed. (Butterworth-Heinemann, 1987); ISBN 0 7506 2767 0.
9. S. BACKHAUS and G. W. SWIFT, "A thermoacoustic-Stirling engine," *Nature* **399**, 335-338 (1999).
10. N. ROTT, "Damped and thermally-driven acoustic oscillations in wide and narrow tubes," *Z. Angew. Math. Phys.* **26**, 230-243 (1969).
11. G. W. SWIFT, *Thermoacoustics: A unifying perspective for some engines and refrigerators* (Acoust. Soc. Am., 2002); ISBN 0735400652.
12. J. W. STRUTT (Lord Rayleigh), "On the circulation of air observed in Kundt's tubes, and on some allied acoustical problems," *Phil. Trans. Royal Soc. London* **175**, 1-21 (1883); *Scientific Papers* (Dover, 1964), Art. 108, Vol. II, pp. 239-257. (A searchable version of *Scientific Papers* is available from the Acoustical Society of American on a CD-ROM, http://www.abdi-ecommerce10.com/asa/c-33-all-products.aspx.)
13. R. A. ALI and S. L. GARRETT, "Heat transfer enhancement through thermoacoustically-driven streaming," *Proc. of Meetings on Acoustics* (POMA) **19**, 030001 (2013); DOI: 10.1121/1.4799202. Joint meeting of the Int. Cong. Acoust. and the Acoust. Soc. Am., 2-7 June 2013, Montreal, Canada.
14. T. B. GABRIELSON, D. L. GARDNER, and S. L. GARRETT, "A simple neutrally buoyant sensor for direct measurement of particle velocity and intensity in water," *J. Acoust. Soc. Am.* **97**(4), 2227-2237 (1995).
15. P. M. MORSE and K. U. INGARD, *Theoretical Acoustics.* (McGraw-Hill, 1968).
16. J. HRISKO, S. L. GARRETT, R. W. M. SMITH, J. A. SMITH, and V. AGARWAL, "The vibroacoustical environment in two nuclear reactors," *J. Acoust. Soc. Am.* **137** (2), 2198 (2015).
17. M. R. SCHROEDER, "The 'Schroeder frequency' revisited," *J. Acoust. Soc. Am.* **99**(5), 3240-3241 (1996).
18. M. LONG, *Architectural Acoustics*. 2nd ed. (Academic Press, 1014); ISBN 978-0-12-398258-2.
19. S. L. GARRETT, *et al., Report on the TAC Sensor Design for the Breazeale Reactor Demonstration*, Idaho Nat'l. Lab. Tech. Rep. INL/LTD-15-34228 (2015).
20. M. R. MOLDOVER, J. P. M. TRUSLER, T. J. EDWARDS, J. B. MEHL, and R. S. DAVIS, "Measurement of the universal gas constant $\Re$ using a spherical acoustic resonator," *J. Res. Nat. Bureau Stand.* **93**, 85-144 (1988).
21 M. R. MOLDOVER, *et al.,* "Acoustic gas thermometry," *Metrologia* **51**, R1-R19 (2014); http://dx.doi.org/10.1088/0026-1394/51/1/R1.
22. R. A. ALI, R. A., S. L. GARRETT, J. A. SMITH, and D. K. KOTTER, "Thermoacoustic thermometry for nuclear reactor monitoring," *IEEE J. Instrumentation & Measurement* **16**(3), 18-25 (2013).